

Dynamic Model of a Bicycle with a Balancer and Its Control

L. Keo*, M. Yamakita*

* Department of Mechanical and Control Engineering
Tokyo Institute of Technology
2-12-1 Ookayama, Meguro-Ku, Tokyo 152-8552, Japan
e-mail: {lychek,yamakita}@ac.ctrl.titech.ac.jp

ABSTRACT

In this paper we present the dynamic model of a bicycle with a balancer and its balancing control. A new configuration balancer that it can be use as a balancer or a flywheel by shifting the center of gravity of the balancer is also presented. This balancer configuration is changed according to the situation of the bicycle system, which corresponds to the change of the dimension of the system. Stabilizing bicycle with the flywheel has better performance than the balancer but it cannot control to shift the bicycle angle to track the desired value, unlike the balancer which can do this motion. The balancer is configured as a flywheel, when disturbances to the system are large, and it will switch to the balancer when we want to shift the bicycle body angle. The simplified model of the bicycle with the balancer is derived from Lagrangian and nonholonomic constraints with respect to translation and rotation relative to the ground plane. The balancing control is derived based on the output-zeroing controller. Numerical simulation and experimental results are shown to verify the effectiveness of the proposed control strategy.

Keywords: Bicycle with Balancer Modeling; Balancing Control; Output-Zeroing; Balancer; Flywheel.

1 Introduction

Research on the stabilization of bicycles has been gained momentum over the last decade in a number of robotic laboratories around the world. Modeling and control of bicycles became a popular topic for researchers in the latter half of the last century. The bicycle literatures are comprehensively reviewed from a control theory perspective in [1] and in [2], which also describe interesting bicycle-related experiments. A. L. Schwab et al. [3] developed the linearized equations of motion for a bicycle as a benchmark and it is suitable for research or application. It is well known that the balancing control of bicycle with steering at zero or slow linear velocity is very difficult [4]. Thus, we are interested to stabilize the bicycle with the balancer that it can allow us to control the bicycle at zero or slow linear velocity.

In this paper, we present the development of a bicycle with a balancer and the balancing control in our laboratory. The first generation of the bicycle with balancer (Fig.1) was developed by M. Yamakita in 2005 [5] by using Lagrange dynamic equations and the balancing control used an output function which is defined by an angular momentum and the new state function is controlled to zero. We reported the experimental study of automatic control of bicycle with a balancer in [6] and [7]. The cooperation control for stabilization of an autonomous bicycle with both steering and balancer was presented in [8] and [9]. The results of balancing bicycle with a steering handlebar and a balancer, it was shown that it has better performance than balancing control of a bicycle with only a balancer. In order to control the bicycle in narrow place, we introduced acrobatic turn via



Figure 1. Bicycle with a balancer system.

wheelie motion that it can allow the bicycle turn on the back wheel at zero linear velocity as shown in Fig.2 and it is presented in [10]. This system is still in the development of experiment and we will report the results in the future. In addition to extending those results to balancing the bicycle,

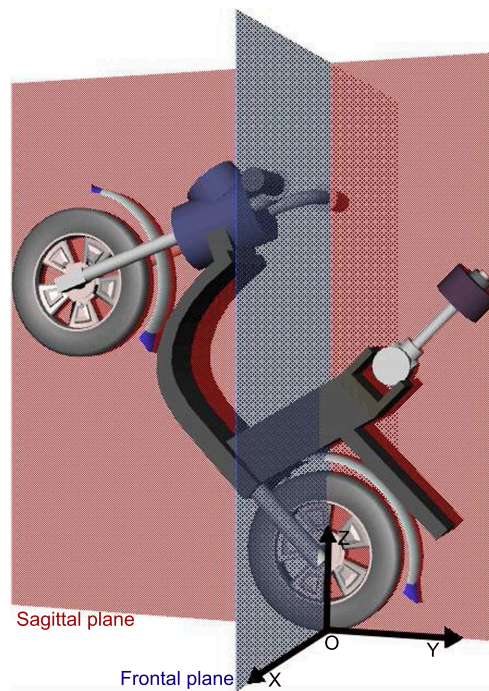


Figure 2. Perform a wheelie on a bicycle with a balancer.

we propose a new balancer configuration [11] for stabilizing of an unmanned bicycle that it shows in Fig.3. In Fig. 3 shows a bicycle experimental setup which has a new balancer configuration on it. This new balancer has two motors, one is a rotating motor which is used to rotate the balancer. The another motor is a linear motor which is used to shift the center gravity of the balancer. With these configurations, we can use the balancer as a flywheel mode (Fig. 4a) or a balancer mode (Fig. 4b). The advantage of the flywheel is to stabilize the bicycle with large region of stability. The advantages of the balancer are to shift the bicycle body from obstacles and to control the bicy-



Figure 3. Bicycle with flywheel balancer hardware.



(a) Flywheel mode



(b) Balancer mode

Figure 4. Flywheel balancer configurations.

cle to follow the trajectory with high speed. This paper is composed of six sections. In section II, we present a simplified dynamic model of the bicycle with the balancer. In section III, we discuss control system design for stabilizing the bicycle. Numerical simulation and experimental results are presented in section IV and V, respectively. The conclusions are summarized in section VI.

2 Bicycle with Balancer Dynamics

In this section, we will present a bicycle with a flywheel balancer model based on an inverted pendulum model. A detailed model of a bicycle is complex since the system has many degrees of freedom. The coordinate system used to analyze the bicycle is defined in Fig. 5. We consider the bicycle as a point mass with two wheel contacts with the ground, and we consider the bicycle and the balancer as a two link system where the first link is the bicycle body with steering and the second link is the balancer. We will define α as the roll angle and β as the balancer angle. The bicycle and the balancer parameters are shown in Table I. These parameters were identified from an experimental setup. The height of the balancer to the center of gravity (h_b) varies from $0m$ to

Table 1. The bicycle with balancer parameters

Parameter descriptions	Par.	Value
Bicycle mass	m	45 kg
Height of the bicycle center of mass	h	0.5 m
Moment inertia of bicycle at COG	I	0.81 kgm^2
Distance between ground and balancer	l	0.87 m
Balancer mass	m_b	11.72 kg
Moment inertia of balancer at COG	I_b	0.49 kgm^2

$0.14m$ and the balancer becomes flywheel when h_b is zero. From [13], we can obtain the bicycle

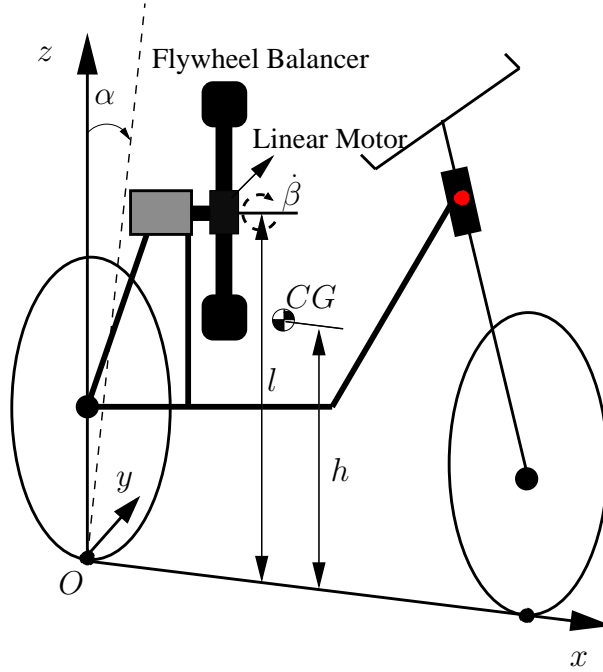


Figure 5. Coordinate system of the bicycle with the balancer.

with flywheel dynamics model as

$$\begin{bmatrix} M_{11} & M_{12} \\ M_{21} & M_{22} \end{bmatrix} \begin{bmatrix} \ddot{\alpha} \\ \ddot{\beta} \end{bmatrix} = \begin{bmatrix} K_1 \\ K_2 \end{bmatrix} + \begin{bmatrix} 0 \\ 1 \end{bmatrix} \tau_b, \quad (1)$$

where τ_b is the balancer torque input and

$$\begin{aligned} M_{11} &= I + I_b + mh^2 + m_b(h_b^2 + l^2 + 2h_b l \cos(\beta)), \\ M_{12} &= M_{21} = I_b + h_b m_b(h_b + l \cos \beta), \\ M_{22} &= I_b + h_b^2 m_b, \\ K_1 &= hmg \sin \alpha + m_b(g(l \sin \alpha + h_b \sin(\alpha + \beta)) \\ &\quad + h_b l \dot{\beta}(2\dot{\alpha} + \dot{\beta}) \sin \beta), \\ K_2 &= h_b m_b(-l\dot{\alpha}^2 \sin \beta + g \sin(\alpha + \beta)). \end{aligned}$$

This gives us a simplified model that we can use to design the controllers for the bicycle stabilization.

3 Balancing Control Algorithm

In this section, we design output-zeroing controller to stabilize the bicycle with flywheel or balancer. The basic idea of output-zeroing controller is that an output function is defined so that the relative degree from input to the output becomes three and the zero dynamic becomes stable. Then, the output-zeroing controller is designed. In this case, a new state is defined then the new output function is easily determined since the angular momentum is integrable for two D.O.F. system.

3.1 Model of two-link system

By projecting the motion of the balancer on YZ plane, the system can be considered as a two-link system (Fig.6). In the two-link model, the bicycle body and steering handlebar consist of the first

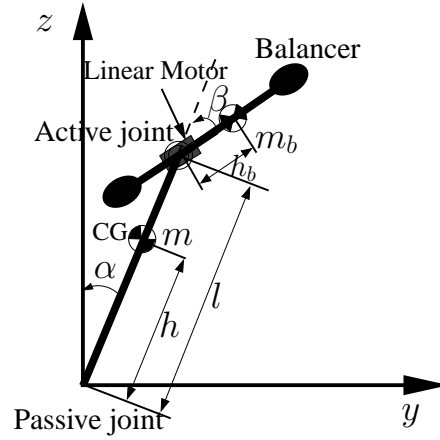


Figure 6. Two-Link System.

link and the balancer with the linear motor is considered as the second link. The control torque for the system is only applied to the second joint of the balancer. We can find the angular momentum L from the first row of equation (1) as

$$\begin{aligned} L &= M_{11}\dot{\alpha} + M_{12}\dot{\beta} \\ &= (d_1 + d_3 + 2d_2 \cos \beta) \dot{\alpha} + (d_3 + d_2 \cos \beta) \dot{\beta}, \end{aligned} \quad (2)$$

where

$$\begin{aligned} d_1 &= I + mh^2 + m_b l^2, \\ d_2 &= m_b l h_b, \\ d_3 &= m_b h_b^2 + I_b, \end{aligned}$$

and it can be easily shown that the time derivative of L just contains a gravity term of K_1 and it is calculated as

$$\dot{L} = e_1 \sin \alpha + e_2 \sin (\alpha + \beta), \quad (3)$$

where

$$\begin{aligned} e_1 &= g(mh + m_b l), \\ e_2 &= gm_b h_b. \end{aligned}$$

Using the angular momentum expressed in (2), a new function p is defined to satisfy the following:

$$L = (d_1 + d_3 + 2d_2 \cos \beta) \dot{p}. \quad (4)$$

From the equation above, p can be determined as

$$p = \alpha + \int_{\beta_0}^{\beta} \frac{d_3 + d_2 \cos \beta}{d_1 + d_3 + 2d_2 \cos \beta} d\beta - C = \alpha + w(\beta), \quad (5)$$

where C is an integral constant and is determined as $p = 0$ when the system is at the upright position. Using L and p , a new coordinate function $q = [p, L, \beta, \dot{\beta}]^T$ can be represented as

$$\begin{bmatrix} \dot{p} \\ \dot{L} \\ \dot{\beta} \\ \ddot{\beta} \end{bmatrix} = \begin{bmatrix} L/H(\beta) \\ G(p, \beta) \\ \dot{\beta} \\ 0 \end{bmatrix} + \begin{bmatrix} 0 \\ 0 \\ 0 \\ 1 \end{bmatrix} u_b, \quad (6)$$

where

$$\begin{aligned} H(\beta) &= d_1 + d_3 + 2d_2 \cos \beta, \\ G(p, \beta) &= e_1 \sin(p - w(\beta)) + e_2 \sin(p - w(\beta) + \beta). \end{aligned}$$

and u_b a new input defined as $u_b := \ddot{\beta}$.

3.2 Output-zeroing controller

For the system (6), an output function y is defined as

$$y = L + a_1 p, \quad (7)$$

where $a_1 \geq 0$ and it is controlled to zero since

$$y = 0 \rightarrow \dot{p} = (-a_1/H)p,$$

this zero dynamics is stable. Since L and p have relative degree of three to the control input, we can easily determine a control input which attains the dynamics of the output function. By taking third derivative of y , we have

$$y^{(3)} = L^{(3)} + a_1 p^{(3)}, \quad (8)$$

$$\ddot{L} = \frac{dG}{dt} = \frac{\partial G}{\partial p} \frac{L}{H} + \frac{\partial G}{\partial \beta} \dot{\beta}, \quad (9)$$

$$L^{(3)} = \frac{d}{dt} \left(\frac{\partial G}{\partial p} \frac{L}{H} \right) + \frac{d}{dt} \left(\frac{\partial G}{\partial \beta} \right) \dot{\beta} + \frac{\partial G}{\partial \beta} u_b, \quad (10)$$

$$\ddot{p} = \frac{G}{H} - \frac{(\partial H / \partial \beta) L}{H^2} \dot{\beta}, \quad (11)$$

$$p^{(3)} = \frac{d}{dt} \left(\frac{G}{H} \right) - \frac{d}{dt} \left(\frac{(\partial H / \partial \beta) L}{H^2} \right) \dot{\beta} - \frac{(\partial H / \partial \beta) L}{H^2} u_b. \quad (12)$$

We can determine a control input which attains the dynamics of the output function as

$$y^{(3)} + a_2 \ddot{y} + a_3 \dot{y} + a_4 y = 0, \quad (13)$$

and y converges to zero asymptotically if $a_2 > 0$, $a_3 > 0$, $a_4 > 0$ are design parameters and they are determined so that the above system is Hurwitz (other robust stabilizing controls of y can be also used). By rearranging the equations from (7) to (13) and we can put it in the form

$$u_b = \left(\frac{\partial G}{\partial \beta} - a_1 \frac{(\partial H / \partial \beta) L}{H^2} \right)^{-1} \left(-\frac{d}{dt} \left(\frac{\partial G}{\partial p} \frac{L}{H} \right) - \frac{d}{dt} \left(\frac{\partial G}{\partial \beta} \right) \dot{\beta} - a_1 \frac{d}{dt} \left(\frac{G}{H} \right) + a_1 \frac{d}{dt} \left(\frac{(\partial H / \partial \beta) L}{H^2} \right) \dot{\beta} - a_2 \ddot{y} - a_3 \dot{y} - a_4 y \right), \quad (14)$$

We can define relationship between $\bar{x} := [y, \dot{y}, \ddot{y}, p] = 0$ and $x := [\alpha, \beta, \dot{\alpha}, \dot{\beta}]$ when a_1 is not zero and a_1 is zero. These relationship can be explained that when a_1 is not zero then $\bar{x} = 0$ implies $x = 0$ locally. However, when a_1 is zero, then $\bar{x} = 0$ implies that α, β , and $\dot{\beta}$ are all zero but $\dot{\alpha}$ is not zero.

4 Numerical Simulation

The simulation is conducted on an Intel Core 2 Duo, 2.2GHz, 2GB RAM computer, and all simulations were performed in MATLAB using a fixed step-size $2ms$. In order to see the robustness of the controller and a new proposed balancer, we add some white noises into the dynamic model and we perform several numerical simulations. The limitation of the control input for the balancer is set to $100[Nm]$. For simulations to be use more easily and more efficiently it is important that a Graphical User Interface (GUI) should be is well functional. MATLAB has the power of handling large amounts of data and performs necessary calculations and is therefore a good platform for a GUI. We create bicycle graphic user interface as in figure 7. The specifications for the most



Figure 7. User interface for a bicycle with a balancer simulator.

important content of the GUI are listed as follows:

- The GUI should handle all necessary preparations before the simulation. Different body of bicycle profiles, steering and balancer are provided.

- Changes to the bicycle with balancer specific parameters, e.g. bicycle total mass m , bicycle length to COG h , distance from ground to the balancer l , horizontal distance from rear wheel contact point to COG c , bicycle wheelbase b , bicycle head angle η , moment inertia of the steering mechanism J_s , bicycle initial angle, bicycle initial position, balancer mass m_b , balancer length to COG h_b , balancer moment inertia I_b , balancer initial angle, ... etc should be possible.
- Selecting modes, balancer, flywheel or flywheel balancer, fix the balancer joint, steering handlebar and back wheel.
- Data and parameter values in specific files must be saved, The GUI should also be able to handle a list of separated data.

The nominal parameters of the bicycle with balancer and range of adjustable values are shown in Table 1. The parameters of the bicycle were identified from an experimental setup.

4.1 Stabilizing the bicycle with a balancer

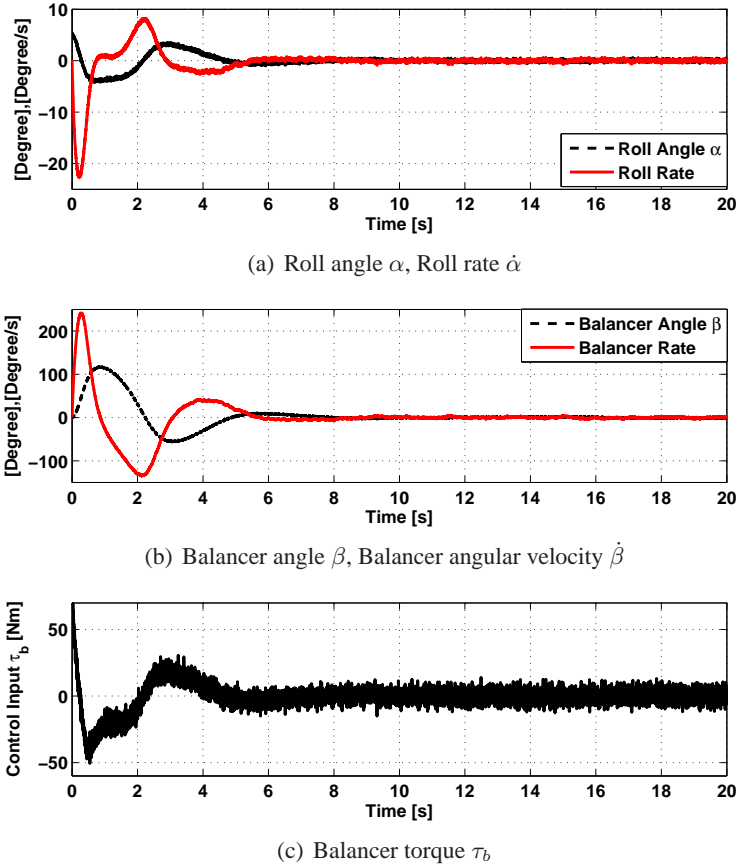
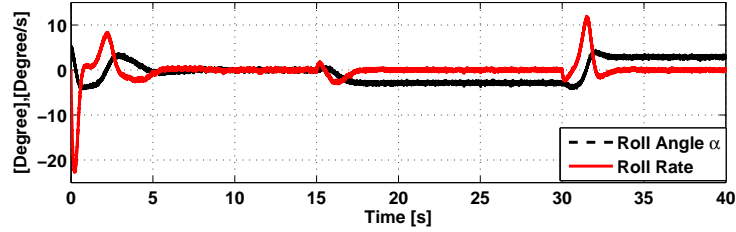


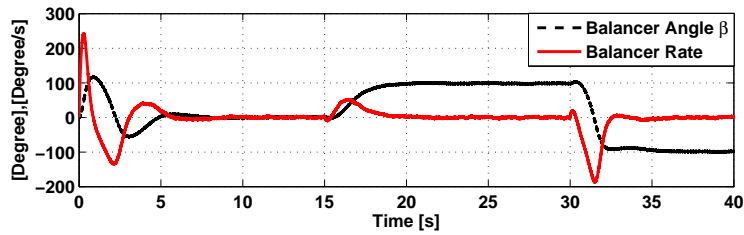
Figure 8. Bicycle stabilization with the balancer

In this simulation, the balancer is used to stabilize the bicycle and the height of the center gravity of the balancer is set to $h_b = 0.14$ [m]. The control parameters are set to $a_1 = 40$, $a_2 = 10$, $a_3 = 15$, and $a_4 = 15$. The initial angles of the bicycle and balancer are set to $\alpha_0 = 5^\circ$ and $\beta_0 = 0^\circ$. Fig.8a shows the roll angle α and roll angular velocity $\dot{\alpha}$ versus t and they converge to the upright position in 5[s]. The balancer angle β and the balancer angular velocity $\dot{\beta}$ are shown in Fig.8b.

The maximum torque to drive the balancer is 55[Nm] and it is shown in Fig.8c. The balancer can stabilize the bicycle within the roll angle 8° . If there are some disturbances that make the bicycle angle larger than 8° , thus the bicycle cannot be controlled by the balancer. The good point of the balancer is that we can control the bicycle angle to track the desired value. Fig.9 shows that the



(a) Roll angle α , Roll angular velocity $\dot{\alpha}$



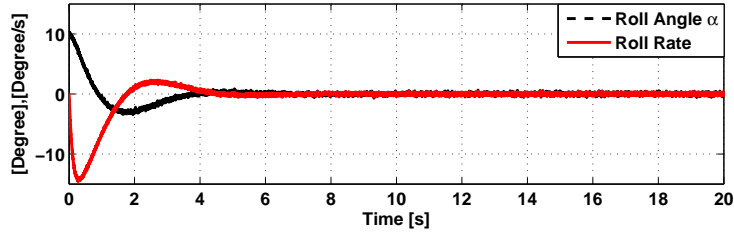
(b) Balancer angle β , Balancer angular velocity $\dot{\beta}$

Figure 9. Tracking desired bicycle angle

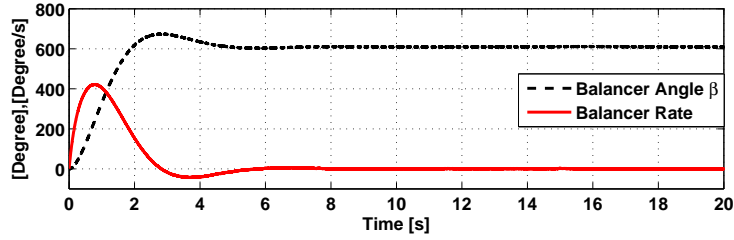
bicycle angle tracks the desired value. Fig.9a shows the roll angle α and roll angular velocity $\dot{\alpha}$ versus t . Fig.9b shows the balancer angle β and balancer angular velocity $\dot{\beta}$ versus t . From these figures, we can see that from the time $t = 15[s]$ to $t = 30[s]$ the bicycle angle tracks the desired value $\alpha_d = -3^\circ$ and from the time $t = 30[s]$ to $t = 40[s]$ the bicycle angle track the desired value $\alpha_d = 3^\circ$. When the bicycle angle tracks to the desire value, the balancer will shift and hold in some position to keep the bicycle stability.

4.2 Stabilizing the bicycle with a flywheel

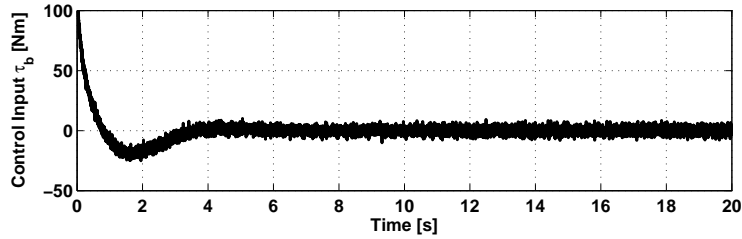
In this simulation, the balancer is configured as the flywheel. Thus, the balancer is rotated around the center of gravity and the height of the balancer to the center of gravity is zero ($h_b = 0$). The control parameters are set to $a_1 = 0$, $a_2 = 10$, $a_3 = 15$, and $a_4 = 15$. The initial angle of the bicycle is set to $\alpha_0 = 10^\circ$. Fig.10a shows the bicycle angle α and angular velocity $\dot{\alpha}$ versus t . It is shown that the bicycle angle is converged to the upright position within 4[s]. Fig.10b shows the flywheel angle β and angular velocity $\dot{\beta}$ versus t . From this figure, we can see that the flywheel angle is not converged to zero, but the flywheel angular velocity is converged to zero. The maximum torque for the flywheel is 85[Nm] that is shown in Fig.10c. When the flywheel angle does not converge to nearly zero, we cannot control the length of the balancer to the balancer mode. If we control the length of the flywheel to the balancer mode when the position of the flywheel is not nearly zero, the balancer will move very fast and the system will become unstable. Thus, we modified the control parameters $a_1 = 40$, $a_2 = 10$, $a_3 = 15$, $a_4 = 15$ to make the balancer angle move around zero. Since the parameter a_1 is not zero, the flywheel angle will slowly converge to zero and it is shown in Fig.11.



(a) Roll angle α , Roll angular velocity $\dot{\alpha}$

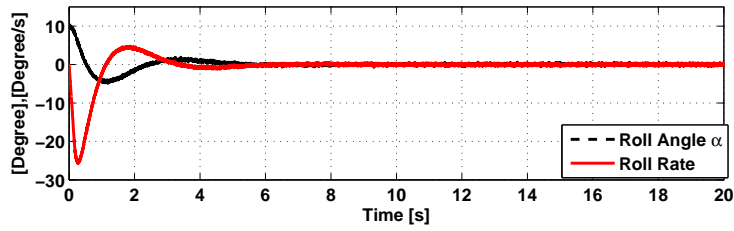


(b) Balancer angle β , Balancer angular velocity $\dot{\beta}$

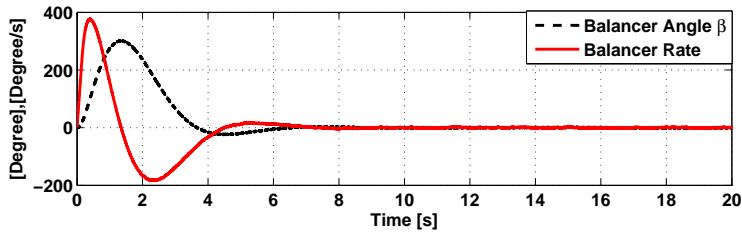


(c) Balancer torque τ_b

Figure 10. Bicycle stabilization with the flywheel and $a_1 = 0$



(a) Roll angle α , Roll angular velocity $\dot{\alpha}$



(b) Balancer angle β , Balancer angular velocity $\dot{\beta}$

Figure 11. Bicycle stabilization with the flywheel and $a_1 = 40$

4.3 Stabilizing the bicycle with flywheel balancer

Since the flywheel and the balancer have different advantages for stabilizing the bicycle, we used both to stabilize the bicycle. The flywheel mode is used when the disturbances to the system are large or the system at startup mode and it will switch to the balancer mode when the system is in the stabilizable region with it. In this simulation, we used the same parameters $a_1 = 40$, $a_2 = 10$, $a_3 = 15$, and $a_4 = 15$ for both flywheel and balancer modes. First, the bicycle system starts up with the flywheel mode and then after some certain of time the system is stable, then we slowly control the position of the balancer h_b from 0 to 0.14[m] as shown in figure 12c. From the time $t = 20$ [s] the bicycle will track the desired bicycle angle value and it is shown in figure 12.

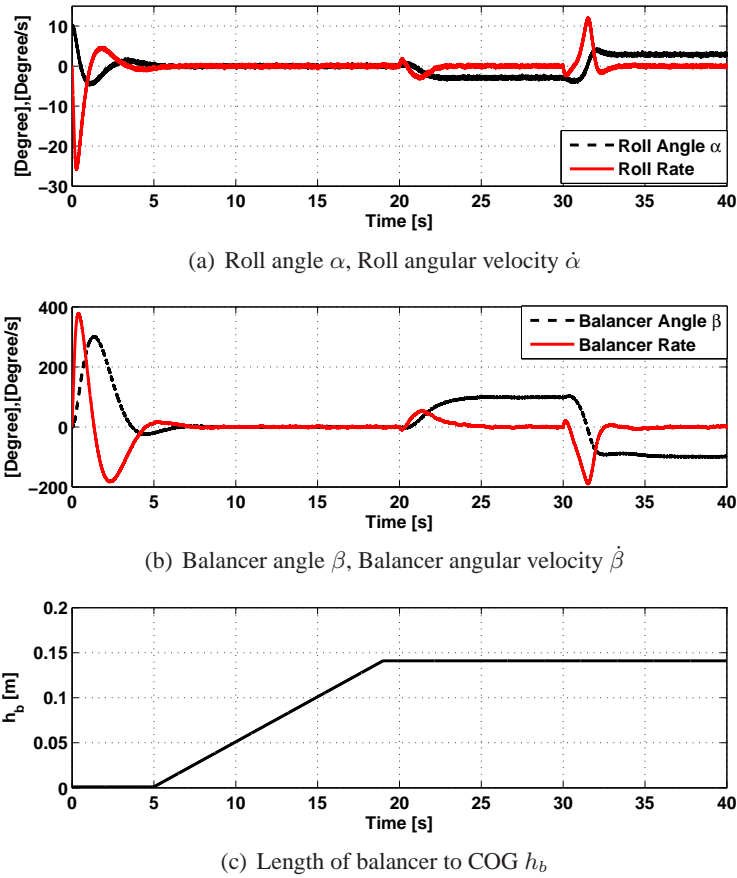


Figure 12. Bicycle stabilization with the flywheel balancer

From this figure, we can see that the new balancer configuration works very well with the output-zeroing controller.

5 Experimental Results

In order to see the validity of the proposed method, some experiments using a real system were conducted. The base system is a commercial available bicycle and we attached a new configuration balancer which can move in a lateral plane and can keep the balance of the bicycle system as shown in figure 3. An inertia measurement unit CROSSBOW IMU 420C is also attached to the bicycle. This sensor detects roll angle and roll angular velocity of the bicycle. The most important part in this bicycle system is control processor unit that it has embedded mother board PC104 from

Advantech model PCM-3350. This system can implement, run XPC target and communication with the host PC. Beside this mother board, we need I/O interface board to communication with actuator, sensor and control panel box. The sampling rate of the controller is 2[ms]. The details of bicycle hardware system is shown in figure 13. In order to implement the bicycle robot, we make

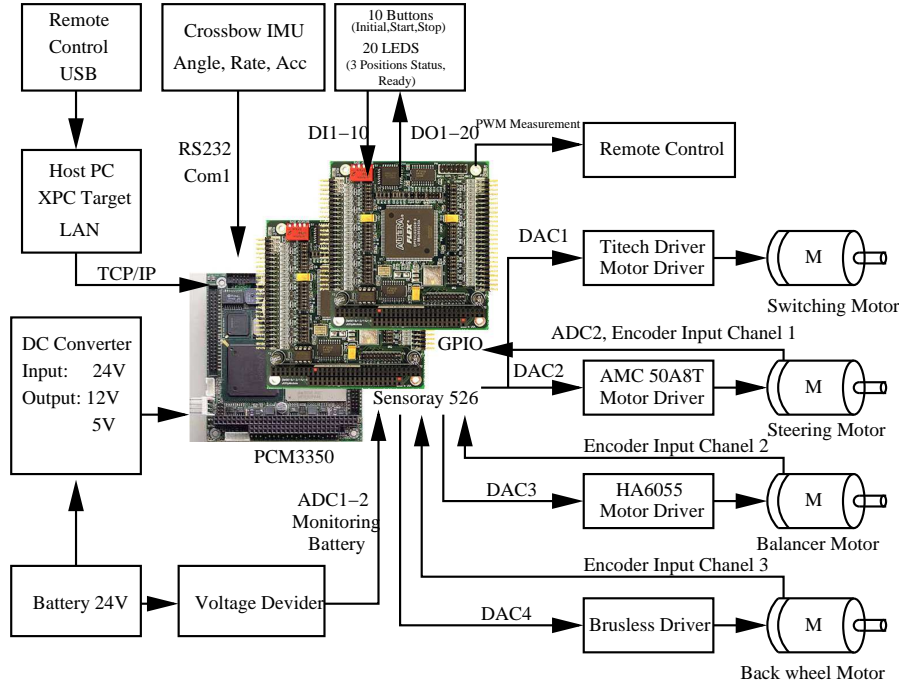


Figure 13. Bicycle hardware system

an control flowchart for safety and prevention from the unstable system during the experiment. This flowchart is shown in figure 14. The control flowchart for the safety and accident prevention have been designed to be simple to use. It consists of a power on switch mounted on the panel box as well as an emergency switch and three switches for enable or disable driver of the motors. When turn on pc, the control system will calibrate the sensors. Once the “Ready” light turn on, the user can simply lift the bicycle and balancer near the upright position. When we push on start button, the bicycle will automatically stabilization at the upright position. In case the bicycle angle is larger than about 15° or steering angle $> 80^\circ$, the control system will automatically switch off the driver motor. The battery voltage permanently monitor by the control system. A couple of minutes prior to their being completely discharged, the battery status on the panel will stay turned on the red light. As soon as the batteries reach their minimal voltage, the PC will turn off automatically. The bicycle robot can be control to move via host PC or via remote control.

5.1 Balancing control of the bicycle robot with balancer

In this experimental study, we perform two different configurations of balancer, first we fix the balancer length to the COG at maximum length $h_b = 0.14[m]$ and then we fix the balancer length to the COG at the middle $h_b = 0.07[m]$. For the first configuration of the balancer, the control parameters are setting as $a_1 = 40, a_2 = 15, a_3 = 10, a_4 = 10$. Figure 15 shows the roll angle and balancer angle versus t . From these results, we can see that the bicycle equilibrium angle is not zero degree that it will make the balancer shift to the reverse side. In the configuration of full length of the balancer, high input torque is required to move the balancer and we need to set the parameter a_1 to be large. If we set the parameter a_1 too large the vibration from the flexible

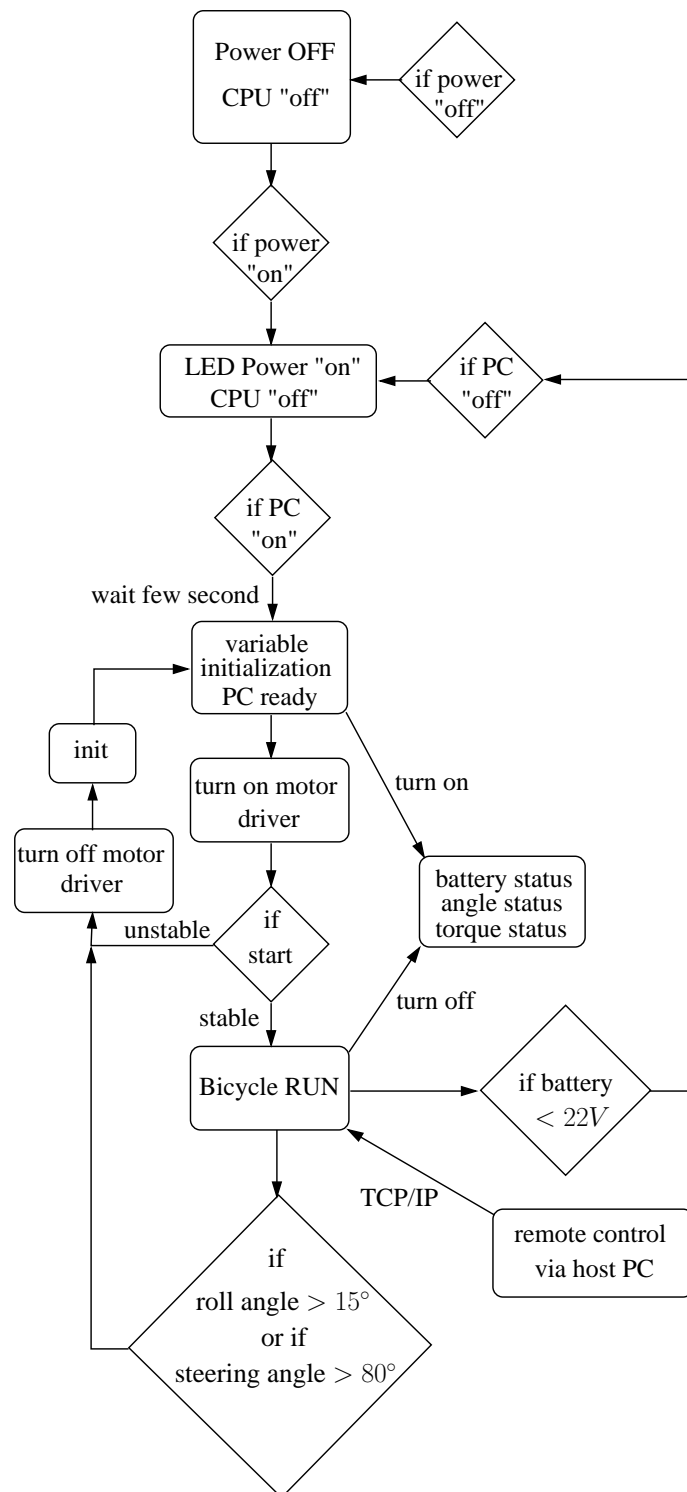


Figure 14. Control flow chart for bicycle robot.

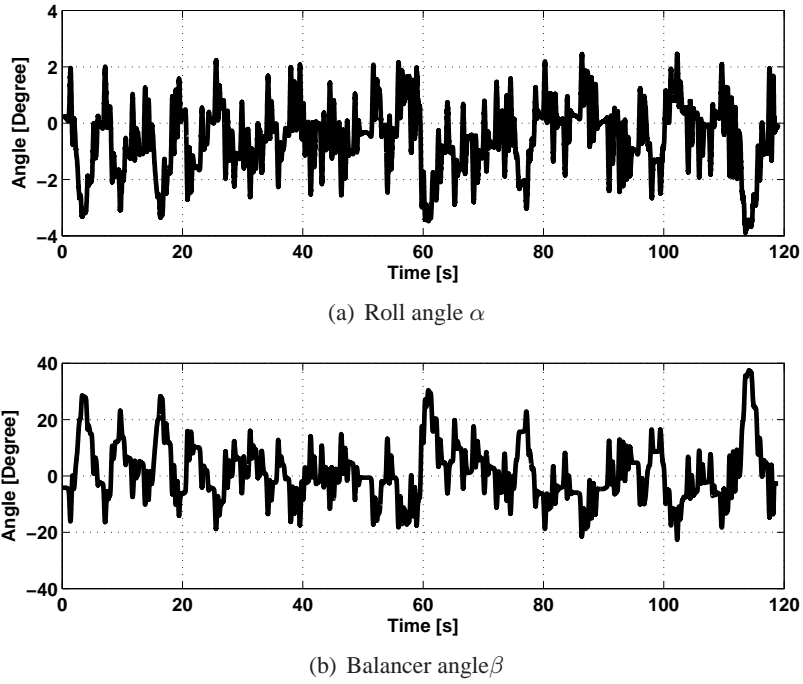


Figure 15. Experimental result of the bicycle stabilization with a balancer mode in full length.

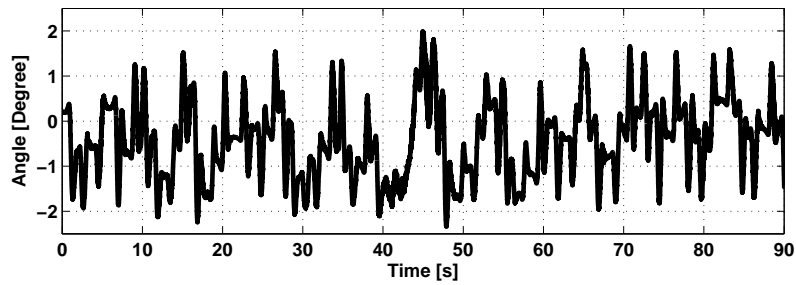
bicycle frame will come out. We need to set an appropriate control parameters depend on the balancer configuration change. Next the control parameters for the second configuration of the balancer are setting as $a_1 = 20, a_2 = 12, a_3 = 10, a_4 = 10$. When the length of the balancer to COG decreased, the parameter a_1 must be decreased to avoid the vibration from the bicycle frame. The amplitude of the roll angle (Figure 16(a)) is also decreased but the balancer moves larger than the full length balancer as show in figure 16(b).

5.2 Balancing control of the bicycle robot with a flywheel

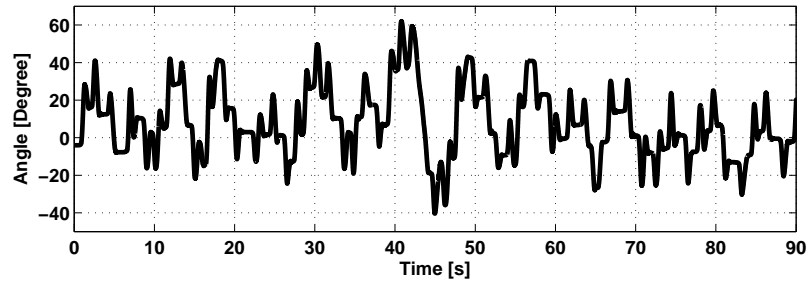
In this subsection, we use an experimental setup for stabilizing the bicycle with flywheel mode. Figure 17 shows the experimental results with the parameters $a_1 = 38, a_2 = 16, a_3 = 14$ and $a_4 = 13$.

5.3 Field test

In disaster areas, road condition is not so good, because many debris and rubbles are on the roads. Rescue robots need to travel under such condition. To determine how high the robot can go over, we made this bicycle robot drive on a bumpy road. The bumpy road has bumps from 5 mm to 60 mm high. The bicycle robot could run smoothly. Figure 18 shows this test. From these experiments, we can see that the bicycle stabilization with flywheel mode works very well. We also attach the movie of this experimental results.



(a) Roll angle α



(b) Balancer angle β

Figure 16. Experimental result of the bicycle stabilization with a balancer mode in half length.

6 Conclusions

The bicycle with balancer model and its balancing control have been presented. A new balancer configuration attaches with the bicycle is fully working and we also validated by experimental setup. From the simulation results, the stabilizing bicycle with flywheel has better performance than balancer but it cannot control to shift the bicycle angle to track the desired value, unlike the balancer which can perform this task. Since the flywheel and the balancer have different advantages for stabilizing the bicycle, we used both to stabilize the bicycle. The flywheel is used when the disturbances to the system are large or at startup mode and it will switch to the balancer when the system is in the stabilizable region with it. Experimental validation of the stabilization of the bicycle with the flywheel balancer and the straight running under bumpy road are also presented. In the future work, the advantages of balancer mode should be tested in several cases, e.g., turning corners with high speed.

REFERENCES

- [1] K. Astrom, R. Klein and A.Lennartsson , "Bicycle Dynamics and Control", *IEEE Control System Magazine*, 25 (2005), pp. 26-47.
- [2] D.J.N. Limebeer and R.S. Sharp , "Bicycles, Motorcycles, and Models,"*IEEE Control System Magazine*, vol. 26, no. 5, pp. 34-61, 2006.
- [3] A. L. Schwab, J. P. Meijaard and J. M. Papadopoulos, "Benchmark Results on the Linearized Equations of Motion of an Uncontrolled Bicycle", *KSME International Journal of Mechanical Science and Technology*, 19 (2005), pp. 292-304.

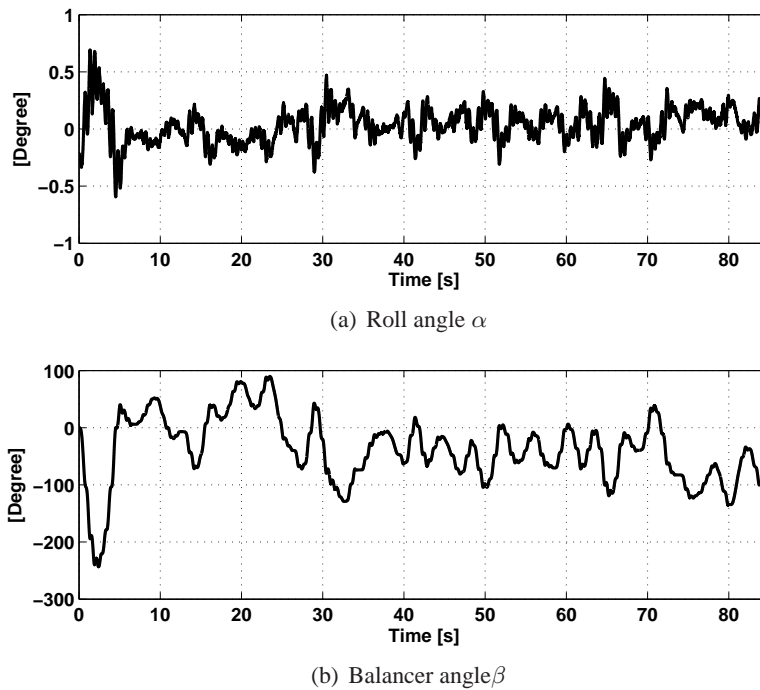


Figure 17. Bicycle stabilization with the flywheel balancer

- [4] R.S. Sharp, "The Stability and Control of Motorcycles," *Journal Mechanical Engineering Science*, vol.13, no. 5, pp.316-329, 1971.
- [5] M. Yamakita and A. Utano, "Automatic Control of Bicycle with a Balancer", *IEEE/ASME Int. Conf. on Advanced Intelligent Mechatronics.*, Monterey, California, USA, 2005, pp. 1245-1249.
- [6] M. Yamakita, A. Utano and K. Sekiguchi, "Experimental Study of Automatic Control of Bicycle with Balancer", *IEEE/RSJ Int. Conf. on Intelligent Robots and Systems*, Beijing, China, 2006, pp. 5606-5611.
- [7] A. Murayama and M. Yamakita, "Development of Autonomous Bike Robot with Balancer", *SICE Annual Conference*, Kagawa, Japan, 2007, pp. 1048-1052.
- [8] L. Keo and M. Yamakita, "Controller Design of an Autonomous Bicycle with Both Steering and Balancer Controls," *IEEE Multi-conference on Systems and Control.*, pp. 1294-1299, 2009.
- [9] L. Keo and M. Yamakita, "Controlling Balancer and Steering for Bicycle Stabilization," *IEEE/RSJ Int. Conf. on Intelligent Robots and Systems.*, pp. 4541-4546, 2009.
- [10] A. Okawa, L. Keo and M. Yamakita, "Realization of Acrobatic Turn via Wheelie for a Bicycle with a Balancer", *Proceeding of IEEE International Conference on Robotics and Automation*, Kobe, Japan, 2009 , pp. 2965-2970 .
- [11] L. Keo and M. Yamakita, "Control of an Unmanned Electric Bicycle with Flywheel Balancer", *Transaction of the Japan Society for Simulation Technology*, 2(2010), pp. 32-38.



Figure 18. Bicycle test under bumpy road.

- [12] J. Yi, D. Song, A. Levandowski and S. Jayasuriya, "Trajectory Tracking and Balance Stabilization Control of Autonomous Motorcycle," *Proceeding IEEE Int. conf. on Robotics and Automation*, pp. 2583-2589, 2006.
- [13] L. Keo and M. Yamakita, "Dynamic Models of a Bicycle with a Balancer System," *The 26th annual conference of the Robotics Society of Japan.*, pp. 43-46, 2008.
- [14] L. Keo and M. Yamakita, "Trajectory Control for an Autonomous Bicycle with Balancer," *IEEE/ASME Int. Conf. on Ad. Intel. Mechatronics.*, pp. 676-681, 2008.
- [15] N.H. Getz, "Dynamic Inversion of Nonlinear Maps with Applications to Nonlinear Control and Robotics," *Ph.D dissertation, Department of Electrical Engineering and Computer Sciences*, University of California at Berkeley, CA, 1995.
- [16] N.H. Getz, J.E. Marsden, "Control for an Autonomous Bicycle," *Proceeding IEEE Int. conf. on Robotics and Automation*, pp. 1397-1402, 1995.